Eradicating catastrophic collapse in interdependent networks via reinforced nodes

Xin Yuan[a,b], Yanqing Hu[c,d,e,1], H. Eugene Stanley[a,b,1], and Shlomo Havlin[f,g]

[a]Center for Polymer Studies, Boston University, Boston, MA 02215; [b]Department of Physics, Boston University, Boston, MA 02215; [c]School of Data and Computer Science, Sun Yat-sen University, Guangzhou 510006, China; [d]School of Mathematics, Southwest Jiaotong University, Chengdu 610031, China; [e]Big Data Research Center, University of Electronic Science and Technology of China, Chengdu 611731, China; [f]Minerva Center, Bar-Ilan University, Ramat-Gan 52900, Israel; and [g]Department of Physics, Bar-Ilan University, Ramat-Gan 52900, Israel

Contributed by H. Eugene Stanley, December 29, 2016 (sent for review April 21, 2016; reviewed by Antonio Coniglio and Michael F. Shlesinger)

In interdependent networks, it is usually assumed, based on percolation theory, that nodes become nonfunctional if they lose connection to the network giant component. However, in reality, some nodes, equipped with alternative resources, together with their connected neighbors can still be functioning after disconnected from the giant component. Here, we propose and study a generalized percolation model that introduces a fraction of reinforced nodes in the interdependent networks that can function and support their neighborhood. We analyze, both analytically and via simulations, the order parameter—the functioning component—comprising both the giant component and smaller components that include at least one reinforced node. Remarkably, it is found that, for interdependent networks, we need to reinforce only a small fraction of nodes to prevent abrupt catastrophic collapses. Moreover, we find that the universal upper bound of this fraction is 0.1756 for two interdependent Erdős–Rényi (ER) networks: regular random (RR) networks and scale-free (SF) networks with large average degrees. We also generalize our theory to interdependent networks of networks (NONs). These findings might yield insight for designing resilient interdependent infrastructure networks.

percolation | interdependent networks | phase transition | collapse

Complex networks often interact and depend on each other to function properly (1–8). Because of interdependencies, these interacting networks may easily suffer abrupt failures and face catastrophic consequences, such as the blackouts of Italy in 2003 and North America in 2008 (3, 4, 6). Thus, a major open challenge arises as how to tackle the vulnerability of interdependent networks. Virtually, many existing theories on the resilience of interacting networks have centered on the formation of the largest cluster (called the giant component) (4, 6, 9–15) and consider only the nodes in the giant component as functional, because all of the small clusters do not have a connection to the majority of nodes, which are in the giant component.

However, in many realistic networks, in case of network component failures, some nodes (which we call here reinforced nodes) and even clusters containing reinforced nodes outside of the giant component can resort to contingency mechanisms or backup facilities to keep themselves functioning normally (16–18). For example, small neighborhoods in a city, when facing a sudden power outage, could use alternative facilities to sustain themselves. Consider also the case where some important internet ports, after their fiber links are cutoff from the giant component, could use satellites (19) or high-altitude platforms (20) to exchange vital information. These possibilities strongly motivate us to generalize the percolation theory (9, 21) to include a fraction of reinforced nodes that are capable of securing the functioning of the finite clusters in which they are located. We apply this framework to study a system of interdependent networks and find that a small fraction of reinforced nodes can avoid the catastrophic abrupt collapse.

In this paper, we develop a mathematical framework based on percolation (4, 6, 12, 13, 22) for studying interdependent networks with reinforced nodes and find exact solutions to the minimal fraction of reinforced nodes needed to eradicate catastrophic collapses. In particular, we apply our framework to study and compare three types of random networks: (*i*) Erdős–Rényi (ER) networks with a Poisson degree distribution [$P(k) = e^{-\langle k\rangle}\langle k\rangle^k/k!$] (23), (*ii*) scale-free (SF) networks with a power law degree distribution [$P(k) \sim k^{-\lambda}$] (24), and (*iii*) regular random (RR) networks with a Kronecker delta degree distribution [$P(k) = \delta_{k,k_0}$]. Here, k stands for the number of connections of a single node. We find the universal upper bound for this minimal fraction to be 0.1756 for two interdependent ER networks with any average degree and SF and RR networks with a large average degree.

Model

Formally, for simplicity and without loss of generality, our model consists of two networks, A and B, with N nodes in each network (Fig. 1). Within network A, the nodes are randomly connected by A links with degree distribution $P_A(k)$, whereas in network B, the nodes are randomly connected by B links with degree distribution $P_B(k)$. In addition, a fraction q_A of nodes in A is randomly dependent (through dependency links) on nodes in network B, and a fraction q_B of nodes in network B is randomly dependent on nodes in network A (25). We also assume that a node from one network depends on no more than one node from the other network, and if a node i in network A is dependent on a node j in network B and j depends on a node l in network A, then $l = i$ [a no-feedback condition (4, 6, 26, 27)]. We denote ρ_A and ρ_B as the fractions of nodes that are randomly chosen as reinforced nodes in network A and network B, respectively. In each network, together with the giant component,

Significance

Percolation theory assumes that only the largest connected component is functional. However, in reality, some components that are not connected to the largest component can also function. Here, we generalize the percolation theory by assuming a fraction of reinforced nodes that can function and support their components, although they are disconnected from the largest connected component. We find that the reinforced nodes reduce significantly the cascading failures in interdependent networks system. Moreover, including a small critical fraction of reinforced nodes can avoid abrupt catastrophic failures in such systems.

Author contributions: X.Y., Y.H., and S.H. designed research; X.Y. and Y.H. performed research; S.H. contributed new reagents/analytic tools; X.Y., H.E.S., and S.H. analyzed data; and X.Y., Y.H., H.E.S., and S.H. wrote the paper.

Reviewers: A.C., University of Naples; and M.F.S., Office of Naval Research.

The authors declare no conflict of interest.

[1]To whom correspondence may be addressed. Email: hes@bu.edu or yanqing.hu.sc@gmail.com.

This article contains supporting information online at www.pnas.org/lookup/suppl/doi:10.1073/pnas.1621369114/-/DCSupplemental.

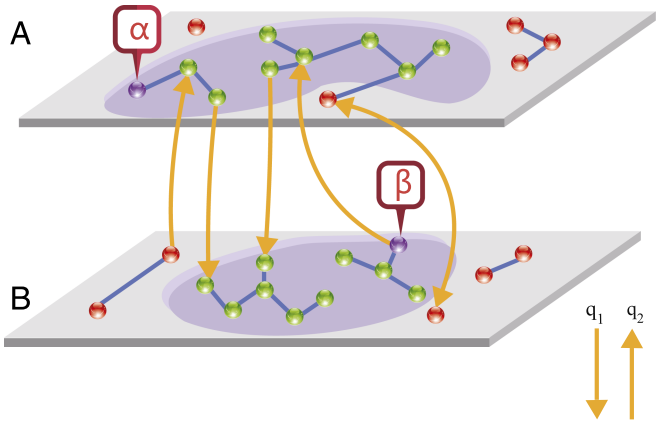

Fig. 1. Demonstration of the model studied here, where two interdependent networks *A* and *B* have gone through cascading failures and reached a steady state. The yellow arrows represent a fraction $q_{A(B)}$ of nodes from network *A*(*B*) depending on nodes from network *B*(*A*) for critical support. Reinforced nodes α and β (purple circles) are nodes that survive and also support their clusters, even if the clusters are not connected to the largest component. Some regular nodes (green circles) survive the cascading failures, whereas some other regular nodes (red circles) fail. Note that the clusters of circles in the shaded purple areas constitute the functioning component studied in our model.

those smaller clusters containing at least one reinforced node make up the functioning component, as shown in Fig. 1. The failure process is initiated by removing randomly a fraction $1-p$ of nodes from each network. Therefore, when nodes from one network fail, their dependent counterparts from the other network must also fail. In this case, an autonomous node (a node that does not need support from the other network) (25) survives if it is connected to a functioning component of its own network; a dependent node n_0 survives if both n_0 and the node that it depends on are connected to their own networks' functioning components.

We introduce the generating function of the degree distribution $G_{A0}(x)=\sum_k P_A(k)x^k$ and the associated branching processes $G_{A1}(x)=G'_{A0}(x)/G'_{A0}(1)$ (14), where $G'_{A0}(x)=\sum_k kP_A(k)x^{k-1}$; similar equations exist to describe network B.

At the steady state, using the probabilistic framework (28–34), we denote x (y) as the probability that a randomly chosen link in network A (B) reaches the functioning component of network A (B) at one of its nodes. Thus, x and y satisfy the following self-consistent equations (*SI Text*, section 2):

$$x = p\,[1-(1-\rho_A)G_{A1}(1-x)]\times \{1-q_A+pq_A[1-(1-\rho_B)G_{B0}(1-y)]\} \quad [1]$$

and

$$y = p\,[1-(1-\rho_B)G_{B1}(1-y)]\times \{1-q_B+pq_B[1-(1-\rho_A)G_{A0}(1-x)]\}. \quad [2]$$

These two equations can be transformed into $x=F_1(p,y)$ and $y=F_2(p,x)$, respectively, which can be solved numerically by iteration with the proper initial values of x and y.

Accordingly, the sizes of the functioning components are determined by (*SI Text*, section 2)

$$P_\infty^A = p[1-(1-\rho_A)G_{A0}(1-x)]\times \{1-q_A+pq_A[1-(1-\rho_B)G_{B0}(1-y)]\} \quad [3]$$

and

$$P_\infty^B = p[1-(1-\rho_B)G_{B0}(1-y)]\times \{1-q_B+pq_B[1-(1-\rho_A)G_{A0}(1-x)]\}. \quad [4]$$

If the system has an abrupt phase transition at $p=p_c^I$, the functions $x=F_1(p,y)$ and $y=F_2(p,x)$ satisfy the condition

$$\frac{\partial F_1(p_c^I,y^I)}{\partial y^I}\cdot\frac{\partial F_2(p_c^I,x^I)}{\partial x^I}=1, \quad [5]$$

namely the curves $x=F_1(p_c^I,y)$ and $y=F_2(p_c^I,x)$ touch each other tangentially at (x^I,y^I) (32, 35).

Results

For a general system of interdependent networks A and B, P_∞^A, P_∞^B, and the existence of p_c^I can be easily determined numerically using Eqs. **1**–**5**. As an example, Fig. 2 shows the excellent agreement between simulation and theory.

However, it is important to find analytic expressions for P_∞^A, P_∞^B, and p_c^I, at least for simpler cases, that can serve as a

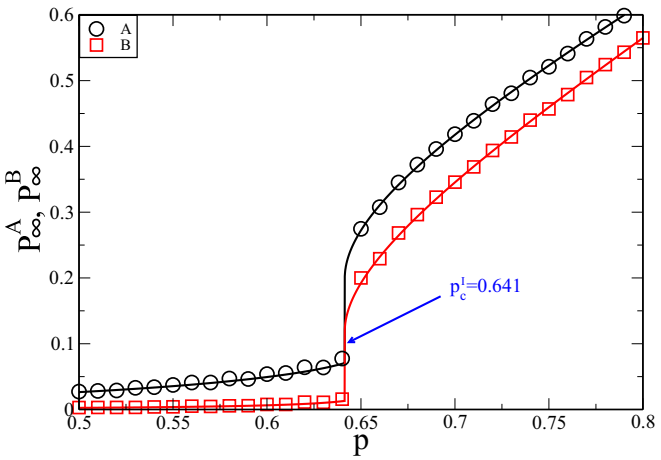

Fig. 2. The sizes of functioning components as a function of p for ER networks with $\rho_A=0.05$, $\rho_B=0.03$, $q_A=0.65$, $q_B=0.95$, $\langle k\rangle_A=4$, and $\langle k\rangle_B=5$. The simulation results (symbols) are obtained from two networks of 10^5 nodes and in good agreement with the theoretical results (solid lines) (Eqs. **3** and **4**). Note that, for $\rho_A\neq 0$ and $\rho_B\neq 0$, network *A*(*B*) always has at least a fraction $p^2\rho_A\rho_B q_A$ ($p^2\rho_A\rho_B q_B$) of nodes functioning after fractions $1-p$ of nodes are removed from both networks.

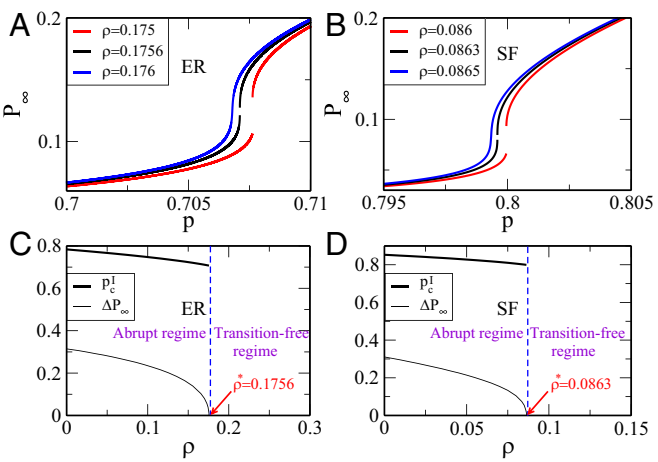

Fig. 3. Percolation properties of symmetric interdependent ER and SF networks. (*A* and *B*) Demonstration of the behavior of P_∞ around ρ^* for (*A*) ER networks with $\langle k\rangle=4$ and $q=1$ and (*B*) SF networks with $P(k)\sim k^{-\lambda}$, $\lambda=2.7$, $k_{\min}=2$, $k_{\max}=2048$, and $q=1$. (*C* and *D*) The abrupt collapse point p_c^I (thick black line) and the jump of the functioning component $\triangle P_\infty$ (thin black lines) at p_c^I as a function of ρ for (*C*) ER and (*D*) SF networks. We find ρ^* for both cases as highlighted in the graphs.

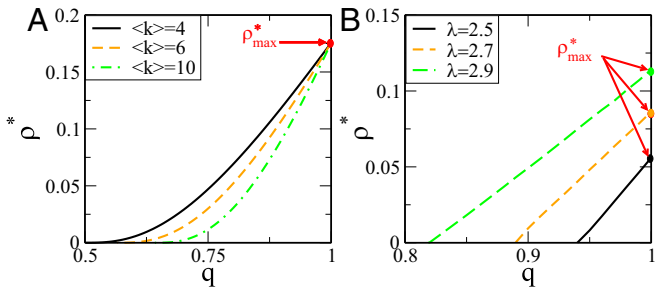

Fig. 4. (*A*) ρ^* As a function of q for symmetric ER networks with different values of $\langle k\rangle$. The results are obtained using Eq. **7**, and these curves converge at the point (1, 0.1756). (*B*) ρ^* As a function of q for symmetric SF networks with $k_{\min}=2$ and different values of λ. The results are obtained from numerical calculations (Eq. **S30** in *SI Text*, section 3). We always have $\rho^*_{\max}$ at $q=1$ corresponding to the fully interdependent scenario.

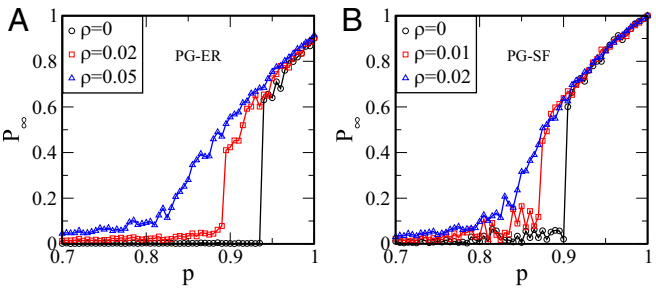

Fig. 6. Percolation transition in real world systems with the introduction of reinforced nodes. (*A*) The circles, squares, and triangles represent simulation results of a system composed of the US PG ($N=4941$ and $\langle k\rangle=2.699$) and an ER network ($N=4941$ and $\langle k\rangle=2.699$) with interdependence strength $q=0.65$ and $\rho=0$, 0.02, 0.05, respectively. (*B*) The circles, squares, and triangles represent simulation results of a system composed of the same PG and an SF network ($N=4941$, $\lambda=2.7$, and $k_{\min}=2$) with interdependence $q=0.65$ and $\rho=0$, 0.01, 0.02, respectively. The symbols are results obtained from a single realization.

benchmark to better understand simulated solutions of more realistic cases. Thus, here, for simplicity, we consider the symmetric case, where $P_A(k)=P_B(k)$, $\rho_A=\rho_B=\rho$, and $q_A=q_B=q$. This symmetry readily implies that $x=y\equiv F(p,x)$, reducing Eqs. **1** and **2** to a single equation. Similarly, it renders $P^A_\infty=P^B_\infty\equiv P_\infty$ and transforms Eq. **5** to $\partial F(p^I_c,x^I)/\partial x^I\cdot dx^I/dx^I=1$ [i.e., $\partial F(p^I_c,x^I)/\partial x^I=1$]. Using Eqs. **1**–**5**, we derive p^I_c and P_∞ rigorously (*SI Text*, section 3).

Surprisingly, we find that, even for a system built with a relatively high dependency coupling, there exists a specific value ρ^* that divides the phase diagram into two regimes. Specifically, if $\rho\le\rho^*$, the system is subject to abrupt transitions; however, if $\rho>\rho^*$, the abrupt percolation transition is absent in the system, because the giant component changes from a first-order phase transition behavior to a second-order phase transition behavior (*SI Text*, section 3). Therefore, ρ^* is the minimum fraction of nodes in each network that needs to be reinforced to make the interdependent system less risky and free from abrupt transitions. Moreover, ρ^* satisfies the condition (*SI Text*, section 3)

$$\frac{dp^I_c}{dx^I}|_{\rho=\rho^*}=0. \qquad [6]$$

Fig. 3 shows the existence of ρ^* for systems of fully interdependent ER networks ($\rho^*\approx0.1756$) and SF networks ($\rho^*\approx0.0863$). Fig. 3 *A* and *B* depicts the dramatic behavior change of the functioning components as ρ increases slightly from under ρ^* to above ρ^*. Fig. 3*C* shows that p^I_c slowly decreases as ρ approaches ρ^* and ceases to exist for $\rho>\rho^*$. We can also see in Fig. 3*D* that

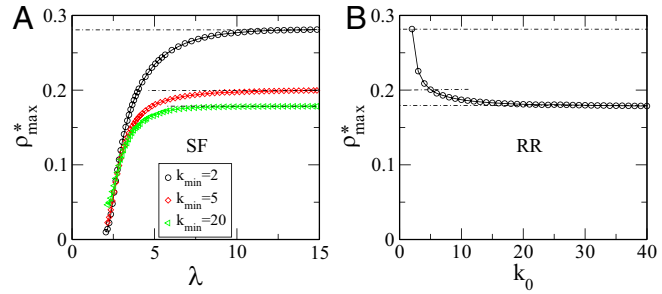

Fig. 5. (*A*) $\rho^*_{\max}$ As a function of λ for two fully interdependent SF networks with the same number of nodes and degree exponent and $k_{\min}=2$ (circles), 5 (diamonds), and 20 (triangles); $\rho^*_{\max}$ has upper limits of 0.282 (circles), 0.201 (diamonds), and 0.181 (triangles) as $\lambda\to\infty$. (*B*) $\rho^*_{\max}$ As a function of k_0 for two fully interdependent RR networks with the same number of nodes and k_0; $\rho^*_{\max}$ approaches 0.1756 as $k_0\to\infty$.

the jump of the functioning component $\triangle P_\infty$ at p^I_c decreases to zero as ρ increases from zero to ρ^*.

We next solve this critical value ρ^* as a function of q and $\langle k\rangle$ for two interdependent ER networks as (*SI Text*, section 3)

$$\rho^*=1-\frac{exp\left\{\frac{1}{2}\left[1-\langle k\rangle(1-q)^2/2q\right]\right\}}{2-\sqrt{\langle k\rangle(1-q)^2/2q}}, \qquad [7]$$

where $q_0\le q\le1$, and q_0 is the minimum strength of interdependence required to abruptly collapse the system (36). If we set $\rho^*=0$ in Eq. **7**, q_0 can be obtained from $\langle k\rangle(1-q_0)^2/2q_0=1$ as $q_0=\left(1+\langle k\rangle-\sqrt{2\langle k\rangle+1}\right)/\langle k\rangle$, as found in refs. 35 and 37. Applying Taylor expansion to Eq. **7** for $q\to q_0$, we get the critical exponent β_1 defined via $\rho^*\backsim(q-q_0)^{\beta_1}$ with $\beta_1=3$.

Hence, for any $q\in[q_0,1]$, we first calculate ρ^* using Eq. **7**; then, p^I_c corresponding to this q and ρ^* can be computed as (*SI Text*, section 3)

$$p^I_c(q,\rho^*)=\left[2-(1-q)\sqrt{\langle k\rangle/2q}\right]/\sqrt{2\langle k\rangle q}, \qquad [8]$$

and the size of the functioning component at this p^I_c is

$$P_\infty(p^I_c)=[1-\langle k\rangle(1-q)^2/2q]/2\langle k\rangle. \qquad [9]$$

The behavior of the order parameter $P_\infty(p)$ near the critical point is defined by the critical exponent β_2, where $P_\infty(p)-P_\infty(p^I_c)\backsim(p-p^I_c)^{\beta_2}$ with $\beta_2=1/3$ if $\rho=\rho^*$ and $\beta_2=1/2$ if $\rho<\rho^*$ (*SI Text*, section 3.1.1) (25). Similar scaling behaviors have been reported in a bootstrap percolation problem (29) and a Fredrickson–Andersen model on Bethe lattice with quenched impurities (38, 39).

In Fig. 4*A*, we plot ρ^* from Eq. **7** as a function q for several different values of $\langle k\rangle$. Interestingly, at $q=1$, namely, for two fully interdependent ER networks, we find, for all mean degrees, the maximum of ρ^* to be

$$\rho^*_{\max}=1-e^{1/2}/2\approx0.1756, \qquad [10]$$

which is independent of $\langle k\rangle$. In Fig. 4*B*, we plot ρ^* as a function of q for several degree exponents λ of SF networks. Here, ρ^* increases as λ increases and takes its maximum $\rho^*_{\max}$ at $q=1$, corresponding to the fully interdependent case, which is the most vulnerable. Thus, if the dependency strength q is unknown, $\rho^*_{\max}$ is the minimal fraction of reinforced nodes that can prevent catastrophic collapse.

Similarly, we obtain $\rho^*_{\max}$ as a function of the degree exponent λ for two fully interdependent SF networks (Fig. 5*A*) and $\rho^*_{\max}$ as a function of k_0 for two fully interdependent RR networks (Fig. 5*B*). Note that, as λ increases, $\rho^*_{\max}$ initially increases but later stabilizes at a value determined by $k_{\min}$ as the degree distribution becomes more homogeneous and its network structure becomes the same as that in an RR network with $k_0 = k_{\min}$ (*SI Text*, section 3.2). For RR networks, as k_0 increases, $\rho^*_{\max}$ initially decreases but later stabilizes at a value close to 0.1756, because at very large k_0, the structure of these RR networks resembles that of ER networks with $\langle k\rangle = k_0$ (*SI Text*, section 3.2).

Next, we solve $\rho^*_{\max}$ of two fully interdependent networks as a function of α, where $\alpha = \langle k\rangle_A/\langle k\rangle_B$ (Fig. S10 in *SI Text*, section 4.1). We find that, in two ER networks, as α increases, $\rho^*_{\max}$ increases and has a maximum at $\alpha = 1$, corresponding to the symmetric case studied above. In the case of RR networks with large k_0, $\rho^*_{\max}$ behaves similarly to its counterpart in ER networks, peaking around $\alpha = 1$ at 0.1756 (Fig. 5*B*). Moreover, in the case of SF networks when $\lambda \in (2, 3]$, $\rho^*_{\max} \le 0.11$; whereas when λ and $k_{\min}$ are relatively large, $\rho^*_{\max}$ will also peak around $\alpha = 1$, with a value close to that obtained in RR networks. Therefore, in the extreme case where λ and $k_{\min}$ are large, SF networks converge to RR networks with $k_0 = k_{\min}$, which further converge to ER networks with $\langle k\rangle = k_0$. Thus, in these extreme cases, there exists a universal $\rho^*_{\max}$ equal to 0.1756 (*SI Text*, section 4.2).

Our approach can be generalized to solve the case of tree-like networks of networks (NONs) (6, 34). For example, we study the symmetric case of an ER NON with n fully interdependent member networks and obtain

$$\rho^*_{\max} = 1 - e^{1-1/n}/n, \qquad [11]$$

which is independent of the average degree $\langle k\rangle$ (*SI Text*, section 3.1.2). This relationship indicates that the bigger n is, the larger $\rho^*_{\max}$ should be, which is consistent with the previous finding that the more networks an NON has, the more vulnerable it will (6).

Test on Empirical Data

We next test our mathematical framework on an empirical network, the US power grid (PG) (40), with the introduction of a small fraction of reinforced nodes. It is difficult to establish the exact structure of the network that the PG interacts with and their interdependencies because of lack of data. However, to get qualitative insight into the problem, we couple the PG with either ER or SF network, which can be regarded as approximations to many real world networks. Our motivation is to test how our model performs in the interdependent networks system with some real world network features. Note that, here, our results present cascading failures caused by structural failures and do not represent failures caused by real dynamics, such as cascading failures caused by overloads, that appear in a PG network system. Fig. 6 compares the mutual percolation of two systems of interdependent networks with the same interdependence strength: PG coupled to a same-sized ER network (Fig. 6*A*) and PG coupled to a same-sized SF network (Fig. 6*B*). As discussed above, for ρ below a certain critical value ρ^*, the systems will undergo abrupt transitions, whereas for ρ above ρ^*, the systems do not undergo any transition at all. We also find that, for the interdependence strength $q = 0.65$ shown here, the ρ^* value of the latter case is very small and close to 0.02 (Fig. 6*B*).

Summary

In summary, we have developed a general percolation framework for studying interdependent networks by introducing a fraction of reinforced nodes at random. We show that the introduction of a relatively small fraction of reinforced nodes, ρ^*, can avoid abrupt collapse and thus, enhance its robustness. By comparing ρ^* in ER, SF, and RR networks, we reveal the close relationship between these network structures in extreme cases and find the universal upper bound for ρ^* to be 0.1756. We also observe improved robustness in systems with some real world network structure features. The framework presented here might offer some useful suggestions on how to design robust interdependent networks.

ACKNOWLEDGMENTS. We thank the financial support of the Office of Naval Research Grants N00014-09-1-0380, N00014-12-1-0548, N62909-16-1-2170, and N62909-14-1-N019; Defense Threat Reduction Agency Grants HDTRA-1-10-1-0014 and HDTRA-1-09-1-0035; National Science Foundation Grants PHY-1505000, CHE-1213217, and CMMI 1125290; Department of Energy Contract DE-AC07-05Id14517; and US–Israel Binational Science Foundation–National Science Foundation Grant 2015781. Y.H. is supported by National Natural Science Foundation of China Grant 61203156, the Hundred-Talent Program of the Sun Yat-sen University, and the Chinese Fundamental Research Funds for the Central Universities Grant 16lgjc84. Financial support was also provided by the European Multiplex and Dynamics and Coevolution in Multilevel Strategic Interaction Games (CONGAS) Projects; the Israel Ministry of Science and Technology with the Italy Ministry of Foreign Affairs; the Next Generation Infrastructure (Bsik); and the Israel Science Foundation. We also thank the Forecasting Financial Crises (FOC) Program of the European Union for support.

1. Rinaldi SM, Peerenboom JP, Kelly TK (2001) Identifying, understanding, and analyzing critical infrastructure interdependencies. *IEEE Control Syst Mag N Y* 21(6):11–25.
2. Little RG (2002) Controlling cascading failure: Understanding the vulnerabilities of interconnected infrastructures. *J Urban Tech* 9(1):109–123.
3. Rosato V, et al. (2008) Modelling interdependent infrastructures using interacting dynamical models. *Int J Crit Infrastruct* 4(1-2):63–79.
4. Buldyrev SV, Parshani R, Paul G, Stanley HE, Havlin S (2010) Catastrophic cascade of failures in interdependent networks. *Nature* 464(7291):1025–1028.
5. Bashan A, Bartsch RP, Kantelhardt JW, Havlin S, Ivanov PCh (2012) Network physiology reveals relations between network topology and physiological function. *Nat Commun* 3:702.
6. Gao J, Buldyrev SV, Stanley HE, Havlin S (2012) Networks formed from interdependent networks. *Nat Phys* 8(1):40–48.
7. Helbing D (2013) Globally networked risks and how to respond. *Nature* 497(7447):51–59.
8. Onnela J-P, et al. (2007) Structure and tie strengths in mobile communication networks. *Proc Natl Acad Sci USA* 104(18):7332–7336.
9. Coniglio A (1982) Cluster structure near the percolation threshold. *J Phys A Math Gen* 15(12):3829–3844.
10. Radicchi F (2015) Percolation in real interdependent networks. *Nat Phys* 11(7):597–602.
11. Reis SDS, et al. (2014) Avoiding catastrophic failure in correlated networks of networks. *Nat Phys* 10(10):762–767.
12. Boccaletti S, et al. (2014) The structure and dynamics of multilayer networks. *Phys Rep* 544(1):1–122.
13. Cohen R, Erez K, Ben-Avraham D, Havlin S (2000) Resilience of the internet to random breakdowns. *Phys Rev Lett* 85(21):4626–4628.
14. Newman ME (2002) Spread of epidemic disease on networks. *Phys Rev E* 66(1 Pt 2): 016128.
15. Cohen R, Havlin S (2010) Complex Networks: Structure, Robustness and Function (Cambridge Univ Press, Cambridge, UK).
16. Jenkins N (1995) Embedded generation. Part 1. *Power Eng J* 9(3):145–150.
17. Pepermans G, Driesen J, Haeseldonckx D, Belmans R, D'haeseleer W (2005) Distributed generation: Definition, benefits and issues. *Energy Policy* 33(6):787–798.
18. Alanne K, Saari A (2006) Distributed energy generation and sustainable development. *Renew Sustain Energ Rev* 10(6):539–558.
19. Henderson TR, Katz RH (1999) Transport protocols for internet-compatible satellite networks. *IEEE J Sel Area Comm* 17(2):326–344.
20. Mohammed A, Mehmood A, Pavlidou F-N, Mohorcic M (2011) The role of High-Altitude Platforms (HAPs) in the global wireless connectivity. *Proc IEEE* 99(11):1939–1953.
21. Vicsek T, Shlesinger MF, Matsushita M (1994) *Fractals in Natural Sciences* (World Scientific, Singapore).
22. Brown A, Edelman A, Rocks J, Coniglio A, Swendsen RH (2013) Monte carlo renormalization-group analysis of percolation. *Phys Rev E* 88(4):043307.
23. Bollobás B (2001) Random Graphs: 1985 (Academic, London).
24. Albert R, Barabási A-L (2002) Statistical mechanics of complex networks. *Rev Mod Phys* 74(1):47–97.
25. Parshani R, Buldyrev SV, Havlin S (2010) Interdependent networks: Reducing the coupling strength leads to a change from a first to second order percolation transition. *Phys Rev Lett* 105(4):048701.
26. Hu Y, Ksherim B, Cohen R, Havlin S (2011) Percolation in interdependent and interconnected networks: Abrupt change from second- to first-order transitions. *Phys Rev E* 84(6 Pt 2):066116.

27. Hu Y, et al. (2013) Percolation of interdependent networks with intersimilarity. *Phys Rev E* 88(5):052805.
28. Son S-W, et al. (2012) Percolation theory on interdependent networks based on epidemic spreading. *Europhys Lett* 97(1):16006.
29. Baxter GJ, Dorogovtsev SN, Goltsev AV, Mendes JFF (2010) Bootstrap percolation on complex networks. *Phys Rev E* 82(1 Pt 1):011103.
30. Baxter GJ, Dorogovtsev SN, Mendes JFF, Cellai D (2014) Weak percolation on multiplex networks. *Phys Rev E* 89(4):042801.
31. Min B, Goh K-I (2014) Multiple resource demands and viability in multiplex networks. *Phys Rev E* 89(4):040802.
32. Feng L, Monterola CP, Hu Y (2015) The simplified self-consistent probabilities method for percolation and its application to interdependent networks. *New J Phys* 17(6):063025.
33. Min B, Lee S, Lee K-M, Goh K-I (2015) Link overlap, viability, and mutual percolation in multiplex networks. *Chaos Solitons Fractals* 72:49–58.
34. Bianconi G, Dorogovtsev SN (2014) Multiple percolation transitions in a configuration model of a network of networks. *Phys Rev E* 89(6):062814.
35. Gao J, et al. (2013) Percolation of a general network of networks. *Phys Rev E* 88(6): 062816.
36. Gao J, et al. (2011) Robustness of a network of networks. *Phys Rev Lett* 107(19): 195701.
37. Parshani R, Buldyrev SV, Havlin S (2011) Critical effect of dependency groups on the function of networks. *Proc Natl Acad Sci USA* 108(3):1007–1010.
38. Ikeda H, Miyazaki K (2015) Fredrickson-Andersen model on Bethe lattice with random pinning. *Europhys Lett* 112(1):16001.
39. de Candia A, Fierro A, Coniglio A (2016) Scaling and universality in glass transition. *Sci Rep* 6:26481.
40. Watts DJ, Strogatz SH (1998) Collective dynamics of 'small-world'networks. *Nature* 393(6684):440–442.
41. Newman MEJ (2010) Networks: An Introduction (Oxford Univ Press, London).
42. Gao J, Buldyrev SV, Havlin S, Stanley HE (2012) Robustness of a network formed by n interdependent networks with a one-to-one correspondence of dependent nodes. *Phys Rev E* 85(6 Pt 2):066134.

Supporting Information

Yuan et al. 10.1073/pnas.1621369114

SI Text

1. Probabilistic Framework for Single Networks with Reinforced Nodes. For a single random network A, we assume its degree distribution $P_A(k)$ fully captures its structural property, and a fraction ρ of nodes is randomly chosen as reinforced nodes. We start by defining a key quantity x, which is the probability to reach the functioning component by following a randomly chosen link to one of its ends (an illustration is in Fig. S1). It will be similarly defined throughout this work and plays a central role in the mathematical analysis.

Suppose we randomly choose a link in network A and find an arbitrary node r by following this link in an arbitrary direction. The probability that node r has degree k is

$$\frac{P_A(k)k}{\sum_k P_A(k)k} = \frac{P_A(k)k}{\langle k_A\rangle}. \quad \textbf{[S1]}$$

There is a probability ρ that r is reinforced and a probability $1-\rho$ that it is not. For node r to be part of the functioning component, at least it must be either a reinforced node, or one of its other $k-1$ outgoing links (other than the link first chosen) leads to the functioning component if node r is not reinforced. By calculating this probability, we can write out the self-consistent Eqs. **S15**, **S29**, and **S32–S35** for x:

$$x = \rho + (1-\rho)\sum_k \frac{P_A(k)k}{\langle k_A\rangle}\left[1-(1-x)^{k-1}\right] = 1-(1-\rho)G_{A1}(1-x), \quad \textbf{[S2]}$$

where ρ is the probability that node r is reinforced, and $1-(1-x)^{k-1}$ is the probability that at least one of the other $k-1$ links of node r leads to the functioning component. Here, $P_A(k)k/\langle k_A\rangle$ is the probability that node r has a degree of k.

Therefore, for a randomly chosen node r, the probability that it is in the functioning component is determined by one of the following conditions: (*i*) it is a reinforced node, or (*ii*) it is not a reinforced node, but at least one of its k links leads to the functioning component. Thus, we define this probability as P_∞ (14, 29–33) and obtain the expression of it as

$$P_\infty = \rho + (1-\rho)\sum_k P_A(k)\left[1-(1-x)^k\right] = 1-(1-\rho)G_{A0}(1-x), \quad \textbf{[S3]}$$

where ρ is the probability that node r is a reinforced node, $1-(1-x)^k$ is the probability that at least one of the k links of node r leads to the functioning component, and $P_A(k)$ is the probability that node r has a degree of k. It is worth noting that P_∞ is also the normalized size of the functioning component.

Furthermore, in the network percolation problem, when a fraction $1-p$ of nodes is removed at random initially from the network (i.e., there is a fraction p nodes remaining), we could apply the above equations with slight modifications. Assuming that the links of the removed nodes are still present on the network, the probability that a randomly selected link leads to the functioning component is the same as before. However, because only a fraction p of the nodes remains in the network, by calculating the probability that the randomly chosen link leads to the functioning component, the self-consistent Eqs. **S33** and **S35** of x in Eq. **S2** become

$$x = p\rho + p(1-\rho)\sum_k \frac{P_A(k)k}{\langle k_A\rangle}\left[1-(1-x)^{k-1}\right] = p\left[1-(1-\rho)G_{A1}(1-x)\right], \quad \textbf{[S4]}$$

where ρ is the probability that node r is a reinforced node, and $1-(1-x)^{k-1}$ is the probability that at least one of the $k-1$ outgoing links of node r leads to the functioning component, same as before. Here, $P_A(k)k/\langle k_A\rangle$ is the probability that node r has a degree of k. The additional multiplication of variable p is because of the fact that only a fraction p of nodes remains in the network after removing a fraction $1-p$ of nodes.

Similarly, the probability that a randomly chosen node is in the functioning component (14, 29–33) is

$$P_\infty = p\left[1-(1-\rho)G_{A0}(1-x)\right]. \quad \textbf{[S5]}$$

Among the functioning component, the biggest contributor is the giant component, which depends on the network structure and bears no influence from reinforced nodes. Thus, we denote by $\tilde{x}$ as the probability to reach the giant component by following a randomly chosen link, and similar to the calculation of x, we can write out the self-consistent equation for $\tilde{x}$:

$$\tilde{x} = p\sum_k \frac{P_A(k)k}{\langle k_A\rangle}\left[1-(1-\tilde{x})^{k-1}\right] = p\left[1-G_{A1}(1-\tilde{x})\right]. \quad \textbf{[S6]}$$

Using $\tilde{x}$, the probability μ_∞ that a randomly chosen node is in the giant component is computed as

$$\mu_\infty = p\sum_k P_A(k)\left[1-(1-\tilde{x})^k\right] = p\left[1-G_{A0}(1-\tilde{x})\right]. \quad \textbf{[S7]}$$

We tested our theory on single random networks by simulations as shown in Fig. S2 with two types of networks: ER and SF. Simulation results agree well with theoretical predictions as shown in Fig. S2. Note that, for ER network, the giant component undergoes a second-order phase transition at $p_c = 1/\langle k\rangle$. It is interesting to note that the threshold is invisible (hidden) when observing only the functioning component. This kind of behavior can be traced to fact that, in the absence of the giant component ($p < p_c$), the network is composed of small clusters, of which those containing reinforced nodes make up a nonzero functioning component. As the occupation probability p increases, more and more small clusters containing reinforced nodes add to the functioning component and enlarge its

size continuously. The giant component appears continuously and linearly from zero as $p \to p_c$, thus growing the functioning component continuously from a nonzero size. As p increases further, the network is predominantly constituted by the giant component and therefore, the functioning component. Similar arguments hold for SF networks (where $p_c = 0$ for $2 < \lambda < 3$).

2. Probabilistic Framework for Interdependent Networks with Reinforced Nodes. For a system of two interdependent networks A and B with the setup described in the text, we denote x (y) as the probability that a randomly chosen link in network A (B) reaches the functioning component of network A (B). Assume now in network A that a random link (solid red line in Fig. S3) is chosen and that a node r (green in Fig. S3) is found following the link. Node r could be either autonomous (i.e., it does not depend on any node in network B) (Fig. S3*A*) or dependent on a single node r' (purple in Fig. S3) in network B (Fig. S3*B*). Thus, this random link leads to the functioning component of network A if either one of the following conditions is met: (E_1) node r is autonomous and connected to the functioning component of network A, or (E_2) node r depends on node r', and they are connected to their own networks' functioning components. Thus, the probability corresponding to E_1 can be calculated as

$$\begin{aligned} P(E_1) &= \left\{ \rho_A + (1-\rho_A) \sum_k \frac{P_A(k)k}{\langle k_A \rangle} \left[1 - (1-x)^{k-1} \right] \right\} \cdot (1 - q_A) \\ &= [1 - (1-\rho_A) G_{A1}(1-x)] \cdot (1 - q_A), \end{aligned} \quad \textbf{[S8]}$$

where $1 - q_A$ is the probability that node r is an autonomous node, and $\{\rho_A + (1-\rho_A)\sum_k P_A(k)k/\langle k_A \rangle [1-(1-x)^{k-1}]\}$ is the probability that node r reached by following the randomly chosen link (solid red line in Fig. S3*A*) belongs to the functioning component of network A. Likewise, the probability corresponding to E_2 can be calculated as

$$\begin{aligned} P(E_2) = q_A \cdot &\left\{ \rho_A + (1-\rho_A) \sum_k \frac{P_A(k)k}{\langle k_A \rangle} \left[1 - (1-x)^{k-1} \right] \right\} \cdot \\ &\left\{ \rho_B + (1-\rho_B) \sum_{k'} P_B(k') \left[1 - (1-y)^{k'} \right] \right\} \\ = q_A \cdot &[1 - (1-\rho_A) G_{A1}(1-x)] \cdot [1 - (1-\rho_B) G_{B0}(1-y)], \end{aligned} \quad \textbf{[S9]}$$

where q_A is the probability that node r depends on a node r' in network B, $\{\rho_A + (1-\rho_A)\sum_k P_A(k)k/\langle k_A \rangle [1-(1-x)^{k-1}]\}$ is the probability that node r reached by following the randomly chosen link (solid red line in Fig. S3*A*) belongs to the functioning component of network A, and $\{\rho_B + (1-\rho_B)\sum_{k'} P_B(k')[1-(1-y)^{k'}]\}$ is the probability that node r' belongs to the functioning component of network B. Note that E_1 and E_2 are mutually exclusive events. Therefore, x can be derived in accordance with the addition rule of probability:

$$x = P(E_1 + E_2) = P(E_1) + P(E_2). \quad \textbf{[S10]}$$

Plugging Eqs. **S8** and **S9** into Eq. **S10**, we obtain x as

$$x = [1 - (1-\rho_A) G_{A1}(1-x)] \{1 - q_A + q_A [1 - (1-\rho_B) G_{B0}(1-y)]\}. \quad \textbf{[S11]}$$

Similarly, we would obtain the probability that a randomly chosen link in B leads to the functioning component of network B as

$$y = [1 - (1-\rho_B) G_{B1}(1-y)] \{1 - q_B + q_B [1 - (1-\rho_A) G_{A0}(1-x)]\}. \quad \textbf{[S12]}$$

Accordingly, a randomly chosen node r of network A resides in the functioning component of network A if either one of the following conditions is satisfied: (E_3) node r is autonomous and connected to the functioning component of network A, or (E_4) node r depends on node r', and they both are connected to their own networks' functioning components.

Hence, the probability corresponding to E_3 can be calculated as

$$\begin{aligned} P(E_3) &= \left\{ \rho_A + (1-\rho_A) \sum_k P_A(k) \left[1 - (1-x)^k \right] \right\} \cdot (1 - q_A) \\ &= [1 - (1-\rho_A) G_{A0}(1-x)] \cdot (1 - q_A), \end{aligned} \quad \textbf{[S13]}$$

where $1 - q_A$ is the probability that node r is an autonomous node, and $\{\rho_A + (1-\rho_A)\sum_k P_A(k)[1-(1-x)^k]\}$ is the probability that node r leads to the functioning component of network A. Likewise, the probability corresponding to E_4 can be calculated as

$$\begin{aligned} P(E_4) = q_A \cdot &\left\{ \rho_A + (1-\rho_A) \sum_k P_A(k) \left[1 - (1-x)^k \right] \right\} \cdot \\ &\left\{ \rho_B + (1-\rho_B) \sum_{k'} P_B(k') \left[1 - (1-y)^{k'} \right] \right\} \\ = q_A \cdot &[1 - (1-\rho_A) G_{A0}(1-x)] \cdot [1 - (1-\rho_B) G_{B0}(1-y)], \end{aligned} \quad \textbf{[S14]}$$

where q_A is the probability that node r depends on a node r' of network B, $\{\rho_A + (1-\rho_A)\sum_k P_A(k)[1-(1-x)^k]\}$ is the probability that node r belongs to the functioning component of network A, and $\{\rho_B + (1-\rho_B)\sum_{k'} P_B(k')[1-(1-y)^{k'}]\}$ is the probability that node r' belongs to the functioning component of network B. Note that E_3 and E_4 are mutually exclusive events. Therefore, the probability P_∞^A that node r is connected to the functioning component of network A can be derived using the addition rule of probability:

$$P_\infty^A = P(E_3 + E_4) = P(E_3) + P(E_4). \quad \textbf{[S15]}$$

Thus, plugging Eqs. **S13** and **S14** into Eq. **S15**, we obtain P_∞^A as

$$P_\infty^A = [1-(1-\rho_A)G_{A0}(1-x)]\{1-q_A+q_A[1-(1-\rho_B)G_{B0}(1-y)]\}, \quad \textbf{[S16]}$$

which is also the normalized size of the functioning component of network A.

Analogously, for network B, we have

$$P_\infty^B = [1-(1-\rho_B)G_{B0}(1-y)]\{1-q_B+q_B[1-(1-\rho_A)G_{A0}(1-x)]\}. \quad \textbf{[S17]}$$

When we randomly remove a fraction $1-p$ of nodes from networks A and B, there is only a fraction p of the nodes left in each network. Hence, of the original probability $x(y)$ that a randomly selected link leads to the functioning component in network $A(B)$, only a fraction p of nodes is actually remaining. It is, thus, easy to write down the new expressions for x and y as

$$\begin{cases} x = p[1-(1-\rho_A)G_{A1}(1-x)]\{1-q_A+pq_A[1-(1-\rho_B)G_{B0}(1-y)]\}, \\ y = p[1-(1-\rho_B)G_{B1}(1-y)]\{1-q_B+pq_B[1-(1-\rho_A)G_{A0}(1-x)]\}. \end{cases} \quad \textbf{[S18]}$$

These two equations can be transformed into $x=F_1(p,y)$ and $y=F_2(p,x)$, which can be solved numerically by iteration with proper initial values of x and y.

Finally, we arrive at the equation for $P_\infty^A(P_\infty^B)$, which is the probability that a randomly selected node in network $A(B)$ is in the functioning component of network $A(B)$:

$$\begin{cases} P_\infty^A = p[1-(1-\rho_A)G_{A0}(1-x)]\{1-q_A+pq_A[1-(1-\rho_B)G_{B0}(1-y)]\}, \\ P_\infty^B = p[1-(1-\rho_B)G_{B0}(1-y)]\{1-q_B+pq_B[1-(1-\rho_A)G_{A0}(1-x)]\}. \end{cases} \quad \textbf{[S19]}$$

Like in a single network, here, we denote $\tilde{x}$ ($\tilde{y}$) as the probability to reach the giant component by following an arbitrarily chosen link in network A (B), and with the values of x and y computed from Eq. **S18**, $\tilde{x}$ and $\tilde{y}$ can be written out as

$$\begin{cases} \tilde{x} = p[1-G_{A1}(1-\tilde{x})]\{1-q_A+pq_A[1-(1-\rho_B)G_{B0}(1-y)]\}, \\ \tilde{y} = p[1-G_{B1}(1-\tilde{y})]\{1-q_B+pq_B[1-(1-\rho_A)G_{A0}(1-x)]\}. \end{cases} \quad \textbf{[S20]}$$

After we obtain the values of $\tilde{x}$ and $\tilde{y}$, the probability μ_∞^A (μ_∞^B) that a randomly chosen node in network A (B) belongs to the giant component of its own network can be computed as

$$\begin{cases} \mu_\infty^A = p[1-G_{A0}(1-\tilde{x})]\{1-q_A+pq_A[1-(1-\rho_B)G_{B0}(1-y)]\}, \\ \mu_\infty^B = p[1-G_{B0}(1-\tilde{y})]\{1-q_B+pq_B[1-(1-\rho_A)G_{A0}(1-x)]\}. \end{cases} \quad \textbf{[S21]}$$

If the system has an abrupt phase transition at $p=p_c^I$, $F_1(p,y)$ and $F_2(p,x)$ satisfy the condition

$$\frac{\partial F_1(p_c^I,y^I)}{\partial y^I}\cdot\frac{\partial F_2(p_c^I,x^I)}{\partial x^I}=1, \quad \textbf{[S22]}$$

namely the curves $x=F_1(p_c^I,y)$ and $y=F_2(p_c^I,x)$ touch each other tangentially at (x^I,y^I).

We test our theory with a system of interdependent ER and SF networks as shown in Fig. S4. Note that simulation results agree well with theoretical predictions, and when the giant components undergo a first-order phase transition at $p=p_c^I$, they will result in a first-order phase transition for their corresponding functioning components at exactly the same value of p_c^I. This first-order phase transition exists because when the giant component suddenly appears from zero to a certain value at $p=p_c^I$, it will abruptly enlarge the size of the functioning component at the same spot as well, which is manifested by a sudden jump of the functioning component. Note also that, at the first-order phase transition point p_c^I, we observe the tangent property of $F_1(p,y)$ and $F_2(p,x)$.

Hence, Eqs. **S18**–**S22** serve as the general framework of the text.

3. Solving Interdependent Networks with Symmetry. In the symmetric case where $\rho_A=\rho_B=\rho$, $q_A=q_B=q$, and $\langle k\rangle_A=\langle k\rangle_B=\langle k\rangle$, we readily have $x=y\equiv F(p,x)$ and $P_\infty^A=P_\infty^B\equiv P_\infty$ as

$$\begin{cases} x = g(x)p+h(x)p^2 \equiv F(p,x); \\ P_\infty^A = p[1-(1-\rho)G_0(1-x)]\{1-q+pq[1-(1-\rho)G_0(1-x)]\} \equiv P_\infty, \end{cases} \quad \textbf{[S23]}$$

where $g(x)=(1-q)[1-(1-\rho)G_1(1-x)]$ and $h(x)=q[1-(1-\rho)G_1(1-x)][1-(1-\rho)G_0(1-x)]$. At the onset of first-order transitions (i.e., $p=p_c^I$), we have $\partial F(p_c^I,x^I)/\partial x^I=1$, namely

$$h'(x^I)(p_c^I)^2+g'(x^I)p_c^I-1=0, \quad \textbf{[S24]}$$

with $h'(x^I)=q(1-\rho)\{G_0'(1-x^I)[1-(1-\rho)G_1(1-x^I)]+G_1'(1-x^I)[1-(1-\rho)G_0(1-x^I)]\}$ and $g'(x^I)=(1-q)(1-\rho)G_1'(1-x^I)$, where $G_0'(1-x^I)$ and $G_1'(1-x^I)$ are derivatives of $G_0(1-x)$ and $G_1(1-x)$ taken with respect to $1-x^I$ as a whole. Solving p_c^I from Eq. **S24**, we have

$$p_c^I(x^I)=\frac{-g'(x^I)+\sqrt{(g'(x^I))^2+4h'(x^I)}}{2h'(x^I)}, \quad \textbf{[S25]}$$

which is a function of x^I. Therefore, x^I must satisfy the equation obtained by substituting p_c^I back into Eq. **S23** as

$$x^I=g(x^I)p_c^I+h(x^I)(p_c^I)^2. \quad \textbf{[S26]}$$

Therefore, we can combine Eqs. **S25** and **S26** to solve for x^I and p_c^I. Note that, if there is more than one solution of x^I, we select the maximal x^I value and the corresponding positive minimal p_c^I value as the physical solution.

As shown in Fig. S5, for $\rho<\rho^*$, there exist two solutions of x^I; however, when $\rho>\rho^*$, there exists no solution of x^I, and when $\rho=\rho^*$, there exists a unique solution of x^I. This critical case takes place when the derivatives of both sides of Eq. **S26** with respect to x^I are equal, i.e.,

$$1=g'(x^I)p_c^I+h'(x^I)(p_c^I)^2+\left[g(x^I)+2h(x^I)p_c^I\right]\frac{dp_c^I}{dx^I}. \quad \textbf{[S27]}$$

From Eq. **S24**, we know that $g'(x^I)p_c^I+h'(x^I)(p_c^I)^2=1$, and therefore, Eq. **S27** could be reduced to

$$0=\left[g(x^I)+2h(x^I)p_c^I\right]\frac{dp_c^I}{dx^I}. \quad \textbf{[S28]}$$

For any $\rho>0$, our definitions of $g(x)$ and $h(x)$ dictate that they are positive for any $x\in[0,1]$, and therefore, $g(x^I)+2h(x^I)p_c^I$ is also positive. Therefore, the determinant that ρ reaches ρ^* turns out to be

$$\frac{dp_c^I}{dx^I}=0. \quad \textbf{[S29]}$$

Using p_c^I obtained from Eq. **S25**, we can further transform the determinant into the following form:

$$g''(x^I)h'(x^I)\left[g'(x^I)-\sqrt{\triangle}\right]+\left[g'(x^I)\sqrt{\triangle}+2h'(x^I)-\triangle\right]h''(x^I)=0, \quad \textbf{[S30]}$$

where $\triangle=(g'(x^I))^2+4h'(x^I)$. Note that Eq. **S30** will be extensively used to obtain ρ^* for different degree distributions $P(k)$ through $g(x)$ and $h(x)$, which are constructed by using the generating functions associated with the degree distribution $P(k)$.

3.1. ER networks. For ER networks, we have $G_0(x)=G_1(x)=e^{\langle k\rangle(x-1)}$ (15, 41), such that $g(x)$ and $h(x)$ can be written out as

$$\begin{cases} g(x)=(1-q)\left[1-(1-\rho)e^{-\langle k\rangle x}\right], \\ h(x)=q\left[1-(1-\rho)e^{-\langle k\rangle x}\right]^2. \end{cases} \quad \textbf{[S31]}$$

Plugging $g(x)$ and $h(x)$ into Eq. **S30**, we can explicitly solve ρ^* and the corresponding x^I as

$$\begin{cases} \rho^*=1-\dfrac{exp\left\{\frac{1}{2}\left[1-\langle k\rangle(1-q)^2/2q\right]\right\}}{2-\sqrt{\langle k\rangle(1-q)^2/2q}}, \\ x^I=\left[1-\langle k\rangle(1-q)^2/2q\right]/2\langle k\rangle, \end{cases} \quad \textbf{[S32]}$$

where q satisfies

$$q\geq q_0=\frac{\left(1+\langle k\rangle-\sqrt{2\langle k\rangle+1}\right)}{\langle k\rangle}. \quad \textbf{[S33]}$$

Apart from the mathematical argument for the existence of the special value ρ^*, we can also see its significance through the percolation properties of the interdependent system. As illustrated in Fig. S6, the sizes of the functioning component (P_∞) and the giant component (μ_∞) are plotted as a function of p for different values of ρ. Note that, if $\rho<\rho^*$, P_∞, and μ_∞ undergo a first-order phase transition at the same p_c^I, then if ρ increases toward ρ^*, it will reduce the jump size of the giant component $\mu_\infty(p_c^I)$. Finally, when $\rho=\rho^*$, $\mu_\infty(p_c^I)$ reduces completely to zero. Therefore, at this transition point, μ_∞ collapses abruptly, occurring from a value very close to zero, which exerts negligible effect on the functioning component. In other words, P_∞ is essentially transitioning continuously at the first-order phase transition point of μ_∞ given $\rho=\rho^*$. Finally, if $\rho>\rho^*$, μ_∞ undergoes a second-order phase transition, which is hidden in the point of view of P_∞, and thus, we call such behaviors of P_∞ transition-free. Thus, $\rho=\rho^*$ is the critical point where the order parameter P_∞ changes from a first-order phase transition behavior to a transition-free behavior, which is also the minimum fraction of reinforced nodes needed in each network to make the system free of catastrophic collapses.

Note that $\rho=\rho^*$ takes its maximum value at $q=1$ with $\rho^*_{max}=1-1/2e^{1/2}$, which is independent of the average degree $\langle k\rangle$. Moreover, $\rho^*=\rho^*(q,\langle k\rangle)$ essentially defines the boundary between the first-order phase transition regime and the transition-free regime. Accordingly, p_c^I on this boundary is obtained as

$$p_c^I=\frac{\left[2-(1-q)\sqrt{\frac{\langle k\rangle}{2q}}\right]}{\sqrt{2\langle k\rangle q}}. \quad \textbf{[S34]}$$

Given x^I and p_c^I, we can get the size of the functioning components of the networks along this boundary line as

$$P_\infty=\left[1-\langle k\rangle(1-q)^2/2q\right]/2\langle k\rangle. \quad \textbf{[S35]}$$

3.1.1. Critical exponent near criticality. For a system of two interdependent ER networks with built-in symmetry, according to Eq. **S23**, $P_\infty(p)$ satisfies the following equation at any p:

$$P_\infty=p(1-q)\left[1-(1-\rho)e^{-\langle k\rangle P_\infty}\right]+p^2q\left[1-(1-\rho)e^{-\langle k\rangle P_\infty}\right]^2, \quad \textbf{[S36]}$$

where because $G_0(1-x)=G_1(1-x)$, we have $x=P_\infty$, and $\langle k\rangle$ is the average degree of the two ER member networks. Solving p from the equation above, we get

$$p=\frac{(q-1)+\sqrt{(q-1)^2+4qP_\infty}}{2q\left[1-(1-\rho)e^{-\langle k\rangle P_\infty}\right]}. \quad \textbf{[S37]}$$

Next, we want to calculate the scaling behavior close to (and above) the critical point

$$p \equiv p_c^I + \varepsilon \tag{S38}$$

$$P_\infty \equiv P_\infty^c + \delta, \tag{S39}$$

when $\varepsilon, \delta \to 0$ and $P_\infty(p) = P_\infty^c$. For this reason, close to the critical point, we have

$$p_c^I + \varepsilon = \frac{(q-1) + \sqrt{(q-1)^2 + 4q(P_\infty^c + \delta)}}{2q\left[1 - (1-\rho)e^{-\langle k\rangle (P_\infty^c + \delta)}\right]} \tag{S40}$$

$$= A\left[1 + C_1\delta + C_2\delta^2 + C_3\delta^3 + \cdots\right], \tag{S41}$$

where $A \equiv (q-1) + \sqrt{(q-1)^2 + 4qP_\infty^c}/2q\left[1 - (1-\rho)e^{-\langle k\rangle P_\infty^c}\right] = p_c^I$, and the linear coefficient is given by

$$C_1 = \frac{(1-q) + \sqrt{(q-1)^2 + 4qP_\infty^c}}{2P_\infty^c\sqrt{(q-1)^2 + 4qP_\infty^c}} - \frac{\langle k\rangle (1-\rho)e^{-\langle k\rangle P_\infty^c}}{1 - (1-\rho)e^{-\langle k\rangle P_\infty^c}}. \tag{S42}$$

Moreover, at the critical point, the derivatives of both sides of Eq. **S36** with respect to P_∞ are equal, i.e.,

$$1 = \langle k\rangle (1-\rho)e^{-\langle k\rangle P_\infty^c}\left\{2(p_c^I)^2 q\left[1 - (1-\rho)e^{-\langle k\rangle P_\infty^c}\right] + p_c^I(1-q)\right\}. \tag{S43}$$

Plugging p_c^I into Eq. **S43**, after some simplification, we would obtain

$$\frac{\langle k\rangle (1-\rho)e^{-\langle k\rangle P_\infty^c}}{1 - (1-\rho)e^{-\langle k\rangle P_\infty^c}} \cdot \frac{2P_\infty^c\sqrt{(1-q)^2 + 4qP_\infty^c}}{(1-q) + \sqrt{(q-1)^2 + 4qP_\infty^c}} = 1. \tag{S44}$$

Combining Eqs. **S42** and **S44**, we can conclude that $C_1 = 0$. From this fact that $C_1 = 0$, we can further calculate the quadratic coefficient C_2 as

$$C_2 = -\frac{\left[(q-1)^2 + 4qP_\infty^c\right]\left[(1-q) + \sqrt{(q-1)^2 + 4qP_\infty^c}\right] + 2q(1-q)P_\infty^c}{2{P_\infty^c}^2\left[(q-1)^2 + 4qP_\infty^c\right]^{\frac{3}{2}}} + \frac{\langle k\rangle^2(1-\rho)e^{-\langle k\rangle P_\infty^c}}{\left[1 - (1-\rho)e^{-\langle k\rangle P_\infty^c}\right]^2}, \tag{S45}$$

which is nonzero unless $\rho = \rho^*$ as determined by Eq. **S32**. We further calculate the value of C_3, and it is always nonzero.

Therefore, if $\rho < \rho^*$, we would have $C_1 = 0$ and $C_2 \neq 0$, and therefore, near the critical point of p_c^I, $\varepsilon \sim \delta^2$, namely $\delta \sim \varepsilon^{1/2}$. Thus, as shown in Fig. S7*A*, the scaling behavior of the functioning component near the first-order transition is characterized by the critical exponent $\beta = 1/2$. Moreover, if $\rho = \rho^*$, we would have $C_1 = C_2 = 0$ and $C_3 \neq 0$, and therefore, near the critical point of p_c^I, $\varepsilon \sim \delta^3$, namely $\delta \sim \varepsilon^{1/3}$. As shown in Fig. S7*B*, the scaling behavior of the functioning component near the first-order transition is characterized by the critical exponent $\beta = 1/3$.

3.1.2. NONs. Our approach can be generalized to solve the case of loopless NONs (6, 42) with the built-in symmetry, where every member network has the same average degree $\langle k\rangle$. For simplicity, we only consider the fully interdependent case here (i.e., $q = 1$). For such an NON formed of n networks, similar to Eq. **S23**, x and P_∞, respectively, satisfy

$$x = p[1 - (1-\rho)G_1(1-x)] \times \{p\left[1 - (1-\rho)G_0(1-x)\right]\}^{n-1}, \tag{S46}$$

and

$$P_\infty = p[1 - (1-\rho)G_0(1-x)]\{p\left[1 - (1-\rho)G_0(1-x)\right]\}^{n-1}. \tag{S47}$$

We tested our theory on a tree-like fully interdependent ER NON system with several values of n. Note that the simulation results agree well with results obtained from theory as shown in Fig. S8*A*. For an ER NON, we can also get a boundary separating the first-order transition regime and the no transition regime. Especially, here, for $q = 1$, we obtain $\rho_{max}^* = 1 - e^{1-1/n}/n$, which is independent of the average degree $\langle k\rangle$ and shown in Fig. S8*B*. For any $n \geq 2$, NON becomes increasingly vulnerable to node failures, which is corroborated here as the bigger n is, the larger ρ_{max}^* will be; hence, more nodes are needed to be reinforced in each network to avoid the risky abrupt transitions.

3.2. Fully interdependent RR and SF networks with symmetry. For $0 < q < 1$ (i.e., the partial interdependent case), we can use Eq. **S30** to numerically solve ρ^* as shown in Fig. 4*B* for SF networks. Here, we are mainly interested in ρ_{max}^*, corresponding to the fully interdependent case (i.e., $q = 1$). Thus, recalling the definitions of $g(x)$ and $h(x)$ in Eq. **S23**, we readily find out that

$$\begin{cases} g(x) = 0, \\ h(x) = \left[1 - (1-\rho)G_0(1-x)\right]\left[1 - (1-\rho)G_1(1-x)\right]. \end{cases} \tag{S48}$$

Therefore, $g'(x^I) = g''(x^I) = 0$ and $h'(x^I) \neq 0$, such that $p_c^I = 1/\sqrt{h'(x^I)}$. Thus, when $\rho = \rho^*$, Eq. **S30** is reduced to

$$h''(x^I) = 0, \tag{S49}$$

i.e.,

$$1-\rho^*_{max}=\frac{G_0''(1-x^I)+G_1''(1-x^I)}{G_0''(1-x^I)G_1(1-x^I)+2G_0'(1-x^I)G_1'(1-x^I)+G_0(1-x^I)G_1''(1-x^I)}. \quad \textbf{[S50]}$$

x^I could be computed from Eq. **S23**:

$$\begin{aligned}x^I&=h(x^I)(p_c^I)^2\\&=\frac{h(x^I)}{h'(x^I)}\\&=\frac{\left[1-mG_1(1-x^I)\right]\left[1-mG_0(1-x^I)\right]}{mG_0'(1-x^I)\left[1-mG_1(1-x^I)\right]+mG_1'(1-x^I)\left[1-mG_0(1-x^I)\right]},\end{aligned} \quad \textbf{[S51]}$$

where $m=1-\rho^*_{max}$.

Thus, Eqs. **S50** and **S51** jointly determine ρ^*_{max} as $\rho^*_{max}=1-m$.

3.2.1. RR networks. For RR networks, we have $P(k)=\delta(k-k_0)$, such that $G_0(x)=x^{k_0}$ and $G_1(x)=x^{k_0-1}$. It is easy to see from Eqs. **S50** and **S51** that ρ^*_{max} depends on k_0. We first solve the case $k_0=2$ with $G_0(1-x^I)=(1-x^I)^2$, $G_0'(1-x^I)=2(1-x^I)$, $G_0''(1-x^I)=2$, $G_1(1-x^I)=1-x^I$, $G_1'(1-x^I)=1$, and $G_1''(1-x^I)=0$. Plugging these quantities into Eq. **S51** first, we get m as

$$m=\frac{1}{3(1-x^I)}. \quad \textbf{[S52]}$$

Then, plugging m into Eq. **S50**, we obtain the equation of x^I as

$$x^I=\frac{2(\frac{2}{3}+\frac{x^I}{3})}{1+\frac{1}{1-x^I}}, \quad \textbf{[S53]}$$

namely $(x^I)^2-8x^I+4=0$ with the physical solution of x^I as $x^I=4-2\sqrt{3}$. Thus, plugging this back into Eq. **S52**, we obtain $\rho^*_{max}=1-m=6-2\sqrt{3}/9\approx 0.282$ as shown in Fig. 5*B*.

For $k_0\geq 3$, we have $G_0(1-x^I)=(1-x^I)^{k_0}$, $G_0'(1-x^I)=k_0(1-x^I)^{k_0-1}$, $G_0''(1-x^I)=k_0(k_0-1)(1-x^I)^{k_0-2}$, $G_1(1-x)=(1-x^I)^{k_0-1}$, $G_1'(1-x^I)=(k_0-1)(1-x^I)^{k_0-2}$, and $G_1''(1-x^I)=(k_0-1)(k_0-2)(1-x^I)^{k_0-3}$, such that

$$m=\frac{k_0(k_0-1)(1-x^I)^{k_0-2}+(k_0-1)(k_0-2)(1-x^I)^{k_0-3}}{2(2k_0-1)(k_0-1)(1-x^I)^{2k_0-3}}, \quad \textbf{[S54]}$$

and similarly, the equation of x^I satisfies

$$x^I=\frac{\left[1-m(1-x^I)^{k_0-1}\right]\left[1-m(1-x^I)^{k_0}\right]}{m(1-x^I)^{k_0-2}\left[k_0(1-x^I)+(k_0-1)\right]-m^2(2k_0-1)(1-x^I)^{2k_0-2}}. \quad \textbf{[S55]}$$

Therefore, for any regular k_0, we can first plug m from Eq. **S54** into Eq. **S55** and get the value of x^I; then, we can plug this x^I value back into Eq. **S54** to get m (i.e., $1-\rho^*_{max}$) as shown in Fig. 5*B*. However, we are also interested in getting the asymptotic form of m when $k_0\to\infty$ to gain more perspective in this system. Here, in the limit of very large k_0, we assume $k_0(k_0-1)\approx(k_0-1)(k_0-2)\approx k_0^2$ and $(2k_0-1)(k_0-1)\approx 2k_0^2$, such that Eq. **S54** reduces to

$$m=\frac{k_0^2\left[(1-x^I)^{1-k_0}+(1-x^I)^{-k_0}\right]}{4k_0^2}=\frac{1}{4}\left[(1-x^I)^{1-k_0}+(1-x^I)^{-k_0}\right]. \quad \textbf{[S56]}$$

Likely assuming $k_0-1\approx k_0$ and $2k_0-1\approx 2k_0$ and with the help of m expressed in Eq. **S56**, we can reduce Eq. **S55** to

$$x^I=\frac{-3(1-x^I)^3+10(1-x^I)^2-3(1-x^I)}{2k_0\left[(1-x^I)^2+2(1-x^I)+1\right]}. \quad \textbf{[S57]}$$

Recall that x^I is a probability in $[0,1]$, and according to Eq. **S57**, as $k_0\to\infty$, $x^I\to 0^+$. More specifically, using Eq. **S57**, we would have

$$\lim_{k_0\to\infty}x^I=\lim_{x^I\to 0^+}\left\{\frac{-3(1-x^I)^3+10(1-x^I)^2-3(1-x^I)}{2k_0\left[(1-x^I)^2+2(1-x^I)+1\right]}\right\}=\frac{1}{2k_0}, \quad \textbf{[S58]}$$

namely $x^I\to 1/2k_0$ as $k_0\to\infty$. Putting this back into Eq. **S56**, we would have

$$\lim_{k_0\to\infty}m=\frac{1}{4}\lim_{k_0\to\infty}\left[\frac{1}{(1-\frac{1}{2k_0})^{k_0-1}}+\frac{1}{(1-\frac{1}{2k_0})^{k_0}}\right]=\frac{1}{2}e^{\frac{1}{2}}, \quad \textbf{[S59]}$$

where we used $\lim_{k_0\to\infty}(1-1/2k_0)^{2k_0}=1/e$. Therefore, $\rho^*_{max}(k_0\to\infty)\approx 1-1/2e^{1/2}$, which is equal to $\rho^*_{max}(\alpha=1)$ of ER networks. This result indicates that, as k_0 increases, the network structure of RR resembles very much that of an ER network with $\langle k\rangle=k_0$.

3.2.2. SF networks. For SF network, the degree distribution is $P(k)=ck^{-\lambda}$, where λ is the degree exponent of the distribution, and $k_{min}\le k\le K$. Here, the degree distribution can be well-approximated by

$$P(k)=\left(\frac{k_{min}}{k}\right)^{\lambda-1}-\left(\frac{k_{min}}{k+1}\right)^{\lambda-1}, \quad \textbf{[S60]}$$

because $k\to\infty$, $P(k)\sim k^{-\lambda}$, and $\sum_{k_{min}}^{K}P(k)=1$. Notice that the average degree $\langle k\rangle$ is

$$\langle k\rangle=k_{min}+\sum_{k_{min}}^{K}\left(\frac{k_{min}}{k+1}\right)^{\lambda-1}, \quad \textbf{[S61]}$$

which is dependent on λ. Thus, we can write out the generating function of the degree distribution $P(k)$ as

$$G_0(x)=\sum_{k_{min}}^{K}\left[\left(\frac{k_{min}}{k}\right)^{\lambda-1}-\left(\frac{k_{min}}{k+1}\right)^{\lambda-1}\right]x^k. \quad \textbf{[S62]}$$

Likely, the generating function for the associated branching processes is

$$G_1(x)=\frac{\sum_{k_{min}}^{K}k\left[\left(\frac{k_{min}}{k}\right)^{\lambda-1}-\left(\frac{k_{min}}{k+1}\right)^{\lambda-1}\right]x^{k-1}}{\langle k\rangle}. \quad \textbf{[S63]}$$

Using $G_0(x)$ and $G_1(x)$, we can further obtain $G_0'(x)$, $G_0^{''}(x)$, $G_1'(x)$, and $G_1^{''}(x)$. Thus, plugging these into Eqs. **S50** and **S51**, we can get ρ^*_{max} for any given λ as shown in Fig. 5*A*.

Moreover, when $\lambda\to\infty$, we note that $\langle k\rangle=k_{min}+\sum_{k_{min}}^{K}(k_{min}/k+1)^{\lambda-1}\approx k_{min}$ and $P(k_{min})=1-(k_{min}/k_{min}+1)^{\lambda-1}\approx 1$, with $P(k)\approx 0$ for $k\ge k_{min}+1$. This calculation means that, now, the SF network becomes extremely like an RR network with $k_0=k_{min}$. Hence, the special value of ρ^*_{max} can be calculated as very close to that obtained in an RR network, namely, $\rho^*_{max}(SF:\lambda\to\infty)\approx\rho^*_{max}(RR:k_0=k_{min})$. This result indicates that, as λ increases, the degree distribution becomes more and more homogeneous, and in the extreme case where $\lambda\to\infty$, the network structure of an SF network is very close to that of an RR network with $k_0=k_{min}$.

4. Solving Fully Interdependent Networks Without Symmetry.

4.1. ER networks. We start with ER networks, because the associated generating functions have the nice property of $G_0(x)=G_1(x)$. We denote ah and bh $(h=1,2,3,...)$ as the average degrees of the fully interdependent ($q_A=q_B=1$) ER networks A and B and readily obtain $G_{A0}(1-x)=G_{A1}(1-x)=e^{-ahx}$ and $G_{B0}(1-y)=G_{B1}(1-y)=e^{-bhy}$. Hence, using Eq. **S18** with $q_A=q_B=1$, we have x and y satisfy

$$x=y=p^2u_Au_B\equiv F(p,x), \quad \textbf{[S64]}$$

where $u_A=1-(1-\rho_A)G_{A0}(1-x)$ and $u_B=1-(1-\rho_B)G_{B0}(1-y)$. With the substitution of x and y, u_A and u_B can be further written as

$$\begin{cases}u_A=1-(1-\rho_A)e^{-ahx}=1-(1-\rho_A)e^{-ahp^2u_Au_B},\\ u_B=1-(1-\rho_B)e^{-bhy}=1-(1-\rho_B)e^{-bhp^2u_Au_B}.\end{cases} \quad \textbf{[S65]}$$

According to the condition of the onset of first-order phase transitions [i.e., $\partial F(p_c^I,x^I)/\partial x^I=1$], we get p_c^I as

$$p_c^I=\frac{1}{\sqrt{ah(1-u_A^I)u_B^I+bh(1-u_B^I)u_A^I}}, \quad \textbf{[S66]}$$

where u_A^I and u_B^I are the specific values that u_A and u_B take at the abrupt transition point. We also denote the value of x at this transition point as x^I. Plugging p_c^I from Eq. **S66** into Eq. **S65**, we can get

$$\begin{cases}u_A^I=1-(1-\rho_A)exp\left\{-\frac{au_A^Iu_B^I}{a(1-u_A^I)u_B^I+b(1-u_B^I)u_A^I}\right\},\\ u_B^I=1-(1-\rho_B)exp\left\{-\frac{bu_A^Iu_B^I}{a(1-u_A^I)u_B^I+b(1-u_B^I)u_A^I}\right\}.\end{cases} \quad \textbf{[S67]}$$

Eq. **S67** indicates that, for the same set of ρ_A and ρ_B, under any given average degrees ah and bh, u_A^I and u_B^I at the corresponding transition point p_c^I are two constant values that only depend on a and b but do not depend on h at all.

Next, we introduce a variable r_c as $r_c=(1-u_A^I/1-\rho_A)^{1/a}=(1-u_B^I/1-\rho_B)^{1/b}=exp\left\{-u_A^Iu_B^I/a(1-u_A^I)u_B^I+b(1-u_B^I)u_A^I\right\}$ to rewrite Eq. **S67** as a single transcendental equation of r_c:

$$r_c=exp\left\{-\frac{\left[1-(1-\rho_A)r_c^a\right]\left[1-(1-\rho_B)r_c^b\right]}{a(1-\rho_A)r_c^a+b(1-\rho_B)r_c^b-(a+b)(1-\rho_A)(1-\rho_B)r_c^{a+b}}\right\}\equiv g(r_c). \quad \textbf{[S68]}$$

Note here that r_c is a variable that does not depend on h at all. Likewise, we have Eq. **S66** recast as a function of r_c:

$$p_c^I=\frac{1}{\sqrt{ah(1-\rho_A)r_c^a+bh(1-\rho_B)r_c^b-(a+b)h(1-\rho_A)(1-\rho_B)r_c^{a+b}}}\equiv p_c^I(h,r_c), \quad \textbf{[S69]}$$

and because $p_c^I \leq 1$, it thus puts a restriction on the parameters as

$$ah(1-\rho_A)r_c^a + bh(1-\rho_B)r_c^b - (a+b)h(1-\rho_A)(1-\rho_B)r_c^{a+b} \geq 1. \quad \textbf{[S70]}$$

Hence, getting r_c from Eq. **S68** and substituting it into Eq. **S69**, we obtain the value of p_c^I for the general case of fully interdependent networks.

Now, we want to derive ρ_{max}^* of such a system with $\rho_A = \rho_B = \rho$, which is a function of ah and bh (i.e., $\rho_{max}^* = \rho_{max}^*(ah, bh)$). This special ρ value corresponds to the case where the derivatives of both sides of Eq. **S68** with respect to r_c are equal, namely

$$1 = \frac{m(a^2 r_c^a + b^2 r_c^b) - 2m^2(a^2+b^2)r_c^{a+b} + m^3 r_c^{a+b}(a^2 r_c^b + b^2 r_c^a)}{\left[m(ar_c^a + br_c^b) - m^2(a+b)r_c^{a+b}\right]^2}, \quad \textbf{[S71]}$$

which can be recast into a cubic function of m with $m = 1 - \rho_{max}^*$.

(*i*) Note that, in our derivation of ρ_{max}^*, we find that ρ_{max}^* does not depend on h, which indicates that

$$\rho_{max}^*(ah, bh) = \rho_{max}^*(a, b) \quad \textbf{[S72]}$$

for any integer h [i.e., $\rho_{max}^*(a, b)$ only depends on the ratio of a and b]. Therefore, given the ratio $\alpha = a/b$, ρ_{max}^* is a function of α only. (*ii*) Also note that, if we interchange a and b in Eq. **S71**, we get the expression exactly unchanged, which means that

$$\rho_{max}^*(a, b) = \rho_{max}^*(b, a). \quad \textbf{[S73]}$$

Of course, this phenomenon results from a very obvious fact that exchanging the average degrees of the two member networks essentially delivers us the same system. Combining these two properties of ρ_{max}^* shown above, we can conclude that

$$\rho_{max}^*(ah, bh) = \rho_{max}^*(a, b) = \rho_{max}^*(b, a) = \rho_{max}^*(bk, ak), \quad \textbf{[S74]}$$

with $k = 1, 2, 3, ...$; thus, Eq. **S74** essentially means $\rho_{max}^*(\alpha) = \rho_{max}^*(1/\alpha)$.

Fig. S9 shows the existence of ρ_{max}^* corresponding to two mutually reciprocal values of α with $\rho_{max}^*(0.4) = \rho_{max}^*(2.5) = 0.156$.

We next solve the dependence of ρ_{max}^* on α, where $\alpha = \langle k \rangle_A / \langle k \rangle_B$ for a system of fully interdependent ER networks. We find that, as α increases, ρ_{max}^* first increases accordingly and then, peaks at $\alpha = 1$, corresponding to the symmetric case studied above, before gradually decreasing as α increases further (Fig. S10*B*). Hence, for any system of interdependent ER networks, we can conclude that ρ_{max}^* will not exceed $\rho_{max}^*(1) \approx 0.1756$.

4.2. RR and SF networks. Now we turn to RR and SF networks where their associated generating functions satisfy $G_0(x) \neq G_1(x)$ unless $x = 0$ or 1. For $q_A = q_B = 1$ and $\rho_A \neq \rho_B$, we have the equation set of x and y as

$$\begin{cases} x = p^2\left[1 - m_A G_{A1}(1-x)\right]\left[1 - m_B G_{B0}(1-y)\right] \\ \quad = p^2 H_1(x, y), \\ y = p^2\left[1 - m_B G_{B1}(1-y)\right]\left[1 - m_A G_{A0}(1-x)\right] \\ \quad = p^2 H_2(x, y); \end{cases}, \quad \textbf{[S75]}$$

$m_A = 1 - \rho_A$ and $m_B = 1 - \rho_B$ for the sake of simplicity. Transforming Eq. **S75** into $x = F_1(p, y)$ and $y = F_2(p, x)$, at the critical point $p = p_c^I$, according to Eq. **S22**, we would have

$$A(p_c^I)^4 + B(p_c^I)^2 - 1 = 0, \quad \textbf{[S76]}$$

where $A = \partial H_1/\partial y^I \cdot \partial H_2/\partial x^I - \partial H_1/\partial x^I \cdot \partial H_2/\partial y^I = m_A m_B\{G'_{A0}(1-x^I)G'_{B0}(1-y^I)[1-m_A G_{A1}(1-x^I)][1-m_B G_{B1}(1-y^I)]-$, $G'_{A1}(1-x^I)G'_{B1}(1-y^I)[1-m_A G_{A0}(1-x^I)][1-m_B G_{B0}(1-y^I)]\}$, $B = \partial H_1/\partial x^I + \partial H_2/\partial y^I = m_A G'_{A1}(1-x^I)[1-m_B G_{B0}(1-y^I)] + m_B G'_{B1}(1-y^I)[1-m_A G_{A0}(1-x^I)]$, and x^I, y^I are the specific values corresponding to this transition point $p = p_c^I$. Note that A is nonzero, because here, $G_0(x) \neq G_1(x)$ and likewise, $G'_0(x) \neq G'_1(x)$. Accordingly, p_c^I can be obtained as

$$p_c^I = \sqrt{\frac{-B + \sqrt{B^2 + 4A}}{2A}}, \quad \textbf{[S77]}$$

which is a function of x^I and y^I. Thus, Eqs. **S75** and **S77** jointly determine the phase transition point for any fully interdependent random networks.

In the case of $m_A = m_B = 1 - \rho$, we want to find the special fraction of reinforced nodes ρ_{max}^* to save the system from the catastrophic failures. To get this ρ_{max}^*, we first put p_c^I obtained from Eq. **S77** into Eq. **S75** to obtain an equation set for x^I, y^I, p_c^I as

$$\begin{cases} x^I = (p_c^I)^2 H_1(x^I, y^I), \\ y^I = (p_c^I)^2 H_2(x^I, y^I). \end{cases} \quad \textbf{[S78]}$$

Notice that Eq. **S78** is the self-consistent equation set for x^I and y^I at the critical point $p = p_c^I$. When ρ is small, there would be no problem finding a solution to Eq. **S78**, because for example, two fully interdependent networks always suffer abrupt collapse under random node removals. However, when ρ gradually increases to ρ_{max}^*, we would reach a point where the solution to Eq. **S78** will suddenly disappear. This scenario corresponds to the case where

$$\frac{dx^I}{dy^I} \cdot \frac{dy^I}{dx^I} = 1, \quad \textbf{[S79]}$$

with

$$\begin{cases} \dfrac{dx^I}{dy^I} = 2p_c^I \cdot \dfrac{dp_c^I}{dy^I} \cdot H_1 + (p_c^I)^2 \cdot \dfrac{dH_1}{dy^I}, \\ \dfrac{dy^I}{dx^I} = 2p_c^I \cdot \dfrac{dp_c^I}{dx^I} \cdot H_2 + (p_c^I)^2 \cdot \dfrac{dH_2}{dx^I}. \end{cases}$$

Thus, using Eqs. **S76** and **S79**, we obtain the determinant that ρ reaches ρ^*_{max} as

$$H_1\frac{\partial p_c^I}{\partial x^I}+H_2\frac{\partial p_c^I}{\partial y^I}=x^I\left(\frac{\partial p_c^I}{\partial x^I}\frac{\partial H_2}{\partial y^I}-\frac{\partial H_2}{\partial x^I}\frac{\partial p_c^I}{\partial y^I}\right)+y^I\left(\frac{\partial H_1}{\partial x^I}\frac{\partial p_c^I}{\partial y^I}-\frac{\partial p_c^I}{\partial x^I}\frac{\partial H_1}{\partial y^I}\right). \quad \textbf{[S80]}$$

According to Eq. **S80**, ρ^*_{max} of two fully interdependent RR networks is shown as a function of α in Fig. S11*A*, where k_0 of network B is fixed at 5, 10, and 20. Note that ρ^*_{max} increases as α increases, and when k_0 is relatively large, it peaks around $\alpha=1$ with $\rho^*_{max}\approx 0.1756$, the same as what we found in two fully interdependent networks in *SI Text*, *Solving Interdependent Networks with Symmetry*. Similarly, from Eq. **S80**, ρ^*_{max} of two fully interdependent SF networks is shown as a function of α in Fig. S11*B*, where k_{min} of network B is fixed at $k_{min}=10$ and $\lambda=2.5, 3, 6, 9$. Note that, as λ increases, the interdependent SF networks become more and more like RR networks, and consequently, ρ^*_{max} peaks around $\alpha=1$, with a value close to that obtained from two RR networks with $k_0=k_{min}$. Therefore, from our discussion above, as $\lambda\to\infty$, we can conclude that two fully interdependent SF networks converge to two fully interdependent RR networks, with k_0 taking the value of k_{min} of the two SF networks; furthermore, as $k_0\to\infty$, these two RR networks converge to two ER networks with ρ^*_{max} peaking at $\alpha=1$ with a value of 0.1756.

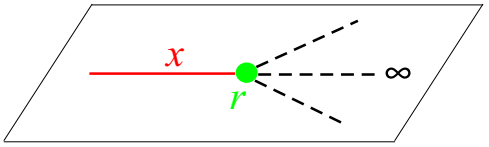

Fig. S1. Definition of *x*. A link (red) is chosen, and a node *r* (green) is found. This node could be a reinforced node with a probability of ρ that ensures its inclusion into the functioning component, or from the three outgoing links (dashed lines) of node *r*, one of them leads to the functioning component (represented by ∞). Because at least one of three outgoing links of *r* leads to the functioning component, the red link leads to the functioning component. Thus, we define the probability of finding such a red link as *x*.

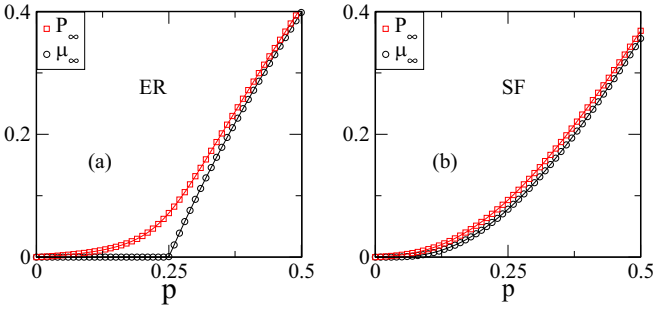

Fig. S2. Size of functioning components and giant components as a function of *p*. (*A*) ER network: $\langle k\rangle=4$, where the functioning component (solid red line) is calculated from Eq. **S5** with $\rho=0.05$, the giant component (solid black line) is computed from Eq. **S7**, and symbols are simulation results obtained from a network size of $N=10^5$ nodes. (*B*) SF network: $P(k)\sim k^{-\lambda}$, $\lambda=2.7$, and $k_{min}=2$, where the functioning component (solid red line) is calculated from Eq. **S5** with $\rho=0.05$, the giant component (solid black line) is computed from Eq. **S7** and symbols are simulation results obtained from a network size of $N=10^5$ nodes.

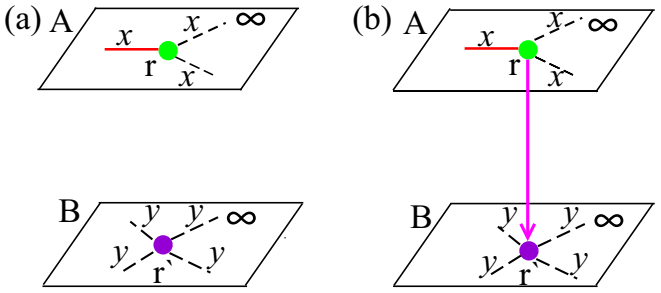

Fig. S3. Definitions of *x* and *y* in interdependent networks. Two networks *A* and *B* both with *N* nodes are constructed in such a way that a fraction q_A of nodes from network *A* depends on nodes in network *B* and a fraction q_B of nodes from network *B* depends on nodes in network *A*. Every link in network *A*(*B*) has the probability *x*(*y*) to lead to the functioning component of network *A*(*B*). A link (solid red line) in network *A* is chosen, and a node *r* (green) is reached following the link. (*A*) Schematic demonstration of the scenario that node *r* is autonomous. (*B*) Schematic demonstration of the scenario that node *r* depends on the node *r*′ in network *B* via the dependency link (solid pink arrow).

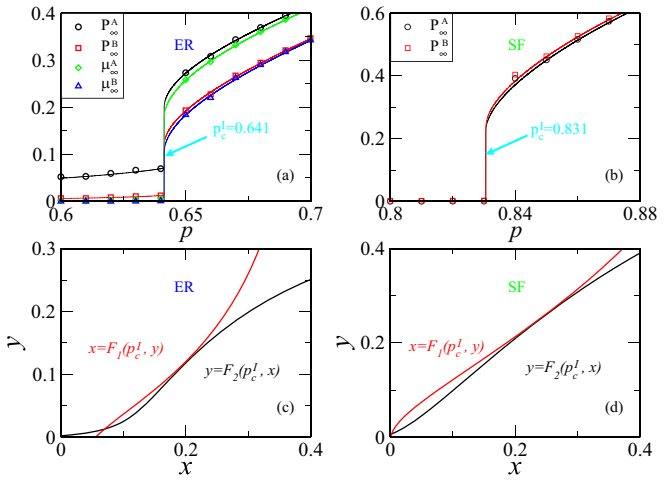

Fig. S4. Percolation transition of interdependent ER networks and interdependent SF networks. (*A*) The sizes of functioning components and the giant components at steady state as a function of p in each network of a system of two interdependent ER networks and (*B*) the sizes of functioning components at steady state as a function of p of the nodes in each network of two interdependent SF networks. All networks are of size 10^5 nodes, and in the ER network scenario, we used $\rho_A = 0.05$, $\rho_B = 0.03$, $q_A = 0.65$, $q_B = 0.95$, $\langle k \rangle_A = 4$, and $\langle k \rangle_B = 5$; however, in the SF network scenario, we used $\rho_A = 0.02$, $\rho_B = 0.03$, $q_A = 1.0$, $q_B = 0.95$, and $\lambda_A = \lambda_B = 2.7$. The simulation results (symbols) are in good agreement with the theoretical results (solid lines) from Eqs. **S19** and **S21**. (*C* and *D*) A characteristic behavior in a first-order percolation transition in coupled networks is that the curves representing $F_1(p, y)$ and $F_2(p, x)$ will tangentially touch each other when p approaches p_c^I. (*C*) For ER networks illustrated in *A* with $p_c^I = 0.641$, the curves of $F_1(p, y)$ and $F_2(p, x)$ touch each other tangentially at $x^I = 0.20$, $y^I = 0.12$, satisfying Eq. **S22**. (*D*) For SF networks illustrated in *B* with $p_c^I = 0.831$, the curves of $F_1(p, y)$ and $F_2(p, x)$ touch each other tangentially at $x^I = 0.25$, $y^I = 0.23$, satisfying Eq. **S22**.

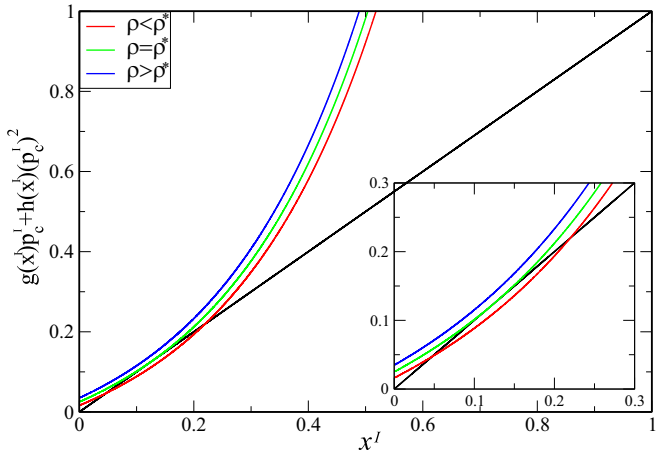

Fig. S5. The left- and right-hand sides of Eq. **S26** are plotted as a straight line (black) and curves (red, green, and blue) for three ρ values, respectively. When $\rho < \rho^*$, there are always two intersections between the line (black) and the curve (red); however, when $\rho = \rho^*$, the line (black) and curve (green) tangentially touch each other at their single intersection; when $\rho > \rho^*$, there is no intersection between the line (black) and the curve (blue) anymore. (*Inset*) A recap of the interesting regime.

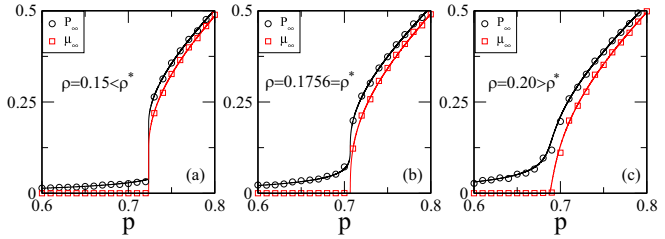

Fig. S6. Percolation properties for symmetric fully interdependent ER networks with (*A*) $\langle k \rangle = 4$, $q = 1$, and $\rho = 0.15 < \rho^*$; (*B*) $\rho = 0.1756 = \rho^*$; or (*C*) $\rho = 0.20 > \rho^*$. Solid lines are from theory (Eqs. **S16** and **S23**), and symbols are simulation results from a network of size $N = 10^5$. Note that, when $\rho \leq \rho^*$, both P_∞ and μ_∞ undergo a first-order phase transition at the same p_c^I. However, when $\rho > \rho^*$, μ_∞ undergoes a second-order transition, and because of the inclusion of smaller clusters, except the giant component, P_∞ is continuous and free of phase transitions.

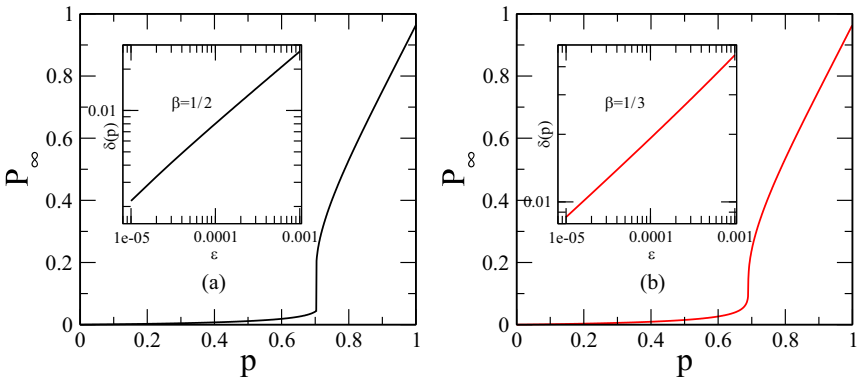

Fig. S7. Scaling behavior near criticality. (*A*) P_∞ as a function of p with $q = 0.9$, $\langle k \rangle = 4$, and $\rho = 0.1$, resulting in $p_c^l = 0.703113$, where the solid line is the result of theoretical calculations. (*Inset*) $P_\infty(p) - P_\infty(p_c^l)$ [denoted as $\delta(p)$] as a function of $p - p_c^l$ (denoted as ϵ), yielding a straight line with a slope of $\beta = 1/2$ in double logarithmic scale. (*B*) P_∞ as a function of p with $q = 0.9$, $\langle k \rangle = 4$, and $\rho = \rho* = 0.119089$, resulting in a $p_c^l = 0.689800$, where the solid line is the result of theoretical calculations. (*Inset*) $P_\infty(p) - P_\infty(p_c^l)$ [denoted as $\delta(p)$] as a function of $p - p_c^l$ (denoted as ϵ), yielding a straight line with a slope of $\beta = 1/3$ in double logarithmic scale.

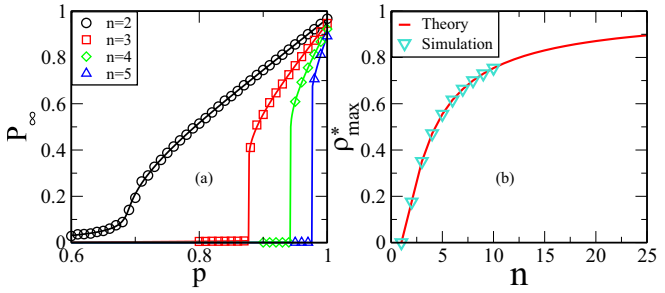

Fig. S8. (*A*) Percolation transition of a tree-like fully ($q = 1$) interdependent ER NON system; P_∞ is shown as a function of p for $\rho = 0.2$ and $\langle k \rangle = 4$ with several different values of n. Here, solid lines are theoretical results obtained from Eq. **S47**, and symbols (◯ for $n = 2$, □ for $n = 3$, ◇ for $n = 4$, and △ for $n = 5$) are simulation results with member networks of 10^5 nodes. Note that, with the same reinforcement fraction $\rho = 0.2$ in each member network, as n increases, the NON system becomes more and more vulnerable. (*B*) ρ^*_{max} Vs. n: the number of ER networks in the ER NON with symmetry where theoretical results are obtained from $\rho^*_{max} = 1 - e^{1-1/n}/n$ and simulation results are obtained from the NON system with member networks of size 10^5. Note that, as n increases, ρ^*_{max} asymptotically reaches one.

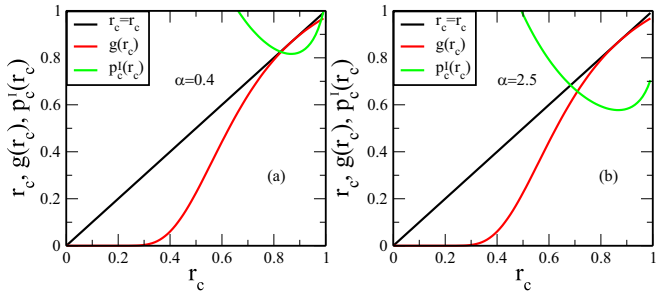

Fig. S9. Schematic shows of the existence of ρ^*_{max} for a system of networks *A* and *B* with different average degrees, where the line $r_c = r_c$ (black) and the curve $r_c = g(r_c)$ (red) tangentially touch each other, and the green curve shows the physically meaningful range of p_c^l: (*A*) $a = 2$, $b = 5$ (i.e., $\alpha = 0.4$ with $\rho^*_{max} = 0.156$) and (*B*) $a = 10$, $b = 4$ (i.e., $\alpha = 2.5$ with $\rho^*_{max} = 0.156$).

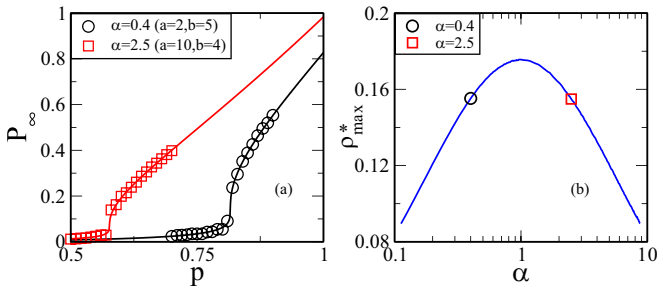

Fig. S10. (*A*) Percolation transition of a fully ($q = 1$) interdependent ER system; P_∞ is shown as function of p for $\rho = 0.156$ with $\alpha = 0.4$ (◯) and $\alpha = 2.5$ (□). Here, solid lines are theoretical results obtained from Eq. **S16** (with $P^A_\infty = P^B_\infty = P_\infty$), and symbols are simulation results with member networks of 10^5 nodes. (*B*) ρ^*_{max} Vs. α, the ratio of $\langle k\rangle_A$ over $\langle k\rangle_B$ in a system of fully interdependent ER networks with $\rho^*_{max}(\alpha) = \rho^*_{max}(1/\alpha)$. Here, theoretical values (solid blue line) are obtained from Eq. **S71**, and symbols are two simulation results (◯ for $\alpha = 0.4$ and □ for $\alpha = 2.5$). Note that $\rho^*_{max}(\alpha)$ is symmetric against the line $\alpha = 1.0$ in this semilogarithmic scale, and it peaks at $\alpha = 1$ with the value of 0.1756.

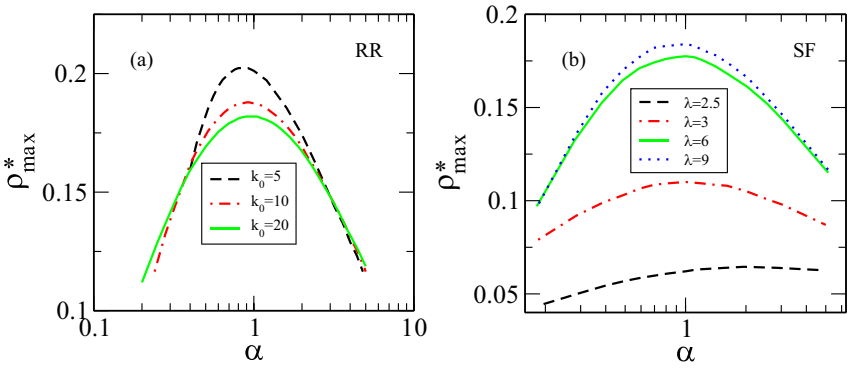

Fig. S11. (*A*) ρ^*_{max} Vs. α: the ratio of k_{0A} over k_{0B} of two fully interdependent RR networks with $k_{0B} = 5$, 10, 20, respectively. (*B*) ρ^*_{max} Vs. α: the ratio of $\langle k\rangle_A$ over $\langle k\rangle_B$ of two fully interdependent SF networks with the lower cutoff of network *B* as $k_{min} = 10$ and $\lambda = 2.5$, 3, 6, 9, respectively.